2021-01

In Search of Durable Sandphobic Thermal/Environmental Barrier Coatings for Rotorcraft Gas Turbine Engines

Murugan, Muthuvel; Ghoshal, Anindya; Walock, Michael; Bravo, Luis; Koneru, Rahul; Jain, Nishan; Mock, Clara; Pepi, Marc; Nieto, Andy; Flatau, Alison...

AIAA

Murugan, Muthuvel, et al. "In Search of Durable Sandphobic Thermal/Environmental Barrier Coatings for Rotorcraft Gas Turbine Engines." AIAA Scitech 2021 Forum. 2021.
http://hdl.handle.net/10945/67542

In Search of Durable Sandphobic Thermal/Environmental Barrier Coatings for Rotorcraft Gas Turbine Engines

Muthuvel Murugan[1]*, Anindya Ghoshal[1], Michael Walock[1], Luis Bravo[1], Rahul Koneru[2], Nishan Jain[2], Clara Mock[1], Marc Pepi[1], Andy Nieto[3], Alison Flatau[2], Sanjay Sampath[4], and Mitch Dorfman[5]

[1]DEVCOM Army Research Laboratory, Aberdeen Proving Ground, MD
[2]University of Maryland, College Park, MD
[3]Naval Postgraduate School, Monterey, CA
[4]SUNY – Stony Brook, Stony Brook, NY
[5]Oerlikon-Metco, Westbury, NY

The objective of this research is to develop new thermal/environmental barrier coatings (T/EBCs) that exhibit greater durability and CMAS (Calcia-Magnesia-Alumino-Silicates) resistance than any of the current state-of-the-art rotorcraft turbine engine coatings. Commercial/Military aircraft engines, especially helicopter engines undergo severe damage to critical components when they need to operate over sandy terrains or volcanic zones. Typical high pressure turbine vanes/blades with current coatings undergo damages that include blade coating wear, sand glazing, Calcia-Magnesia-Alumina-Silicates (CMAS) attack, oxidation, plugged cooling holes, all of which can cause rapid engine performance loss and in severe cases ending up in loss of aircraft. Design of novel T/EBCs for high temperature operation is presented in this paper based on ongoing work in understanding the fundamental governing parameters affecting CMAS adhesion, build-up, and chemical attack. The paper intends to report specific objectives and findings obtained thus far from an ambitious T/EBC research program funded by OSD's Strategic Environmental Research and Development Program (SERDP). Systematic sand-phobic development research efforts and methodologies from modeling to engine relevant high-temperature environmental test evaluations are described in this paper to innovate improved T/EBCs for both Ni-superalloy based substrates and emerging SiC-SiC Ceramic Matrix Composite (CMC) based substrates.

I. Nomenclature

APS	=	Air Plasma Spray
ARL	=	DEVCOM Army Research Laboratory
CFD	=	Computational Fluid Dynamics
CMAS	=	Calcia-Magnesia-Alumino-Silicates
DEVCOM	=	U.S. Army Combat Capabilities Development Command
DoD	=	Department of Defense
FOD	=	Foreign Object Damage
GTEs	=	Gas Turbine Engines
HPT	=	High Pressure Turbine
LE	=	Leading Edge of vane or blade
Ma	=	Mach number
OSD	=	Office of the Secretary of Defense
RE	=	Rare Earth
TBC	=	Thermal Barrier Coatings
T/EBC	=	Thermal/Environmental Barrier Coatings
TE	=	Trailing Edge of vane or blade

* Corresponding Author, Research Aerospace Engineer, U.S. Army Research Laboratory, AIAA Associate Fellow

II. Introduction

Thermal barrier coatings (TBCs) made of low-thermal conductivity ceramics are currently used in gas turbine engines to provide thermal protection to turbine blades from the hot gas stream [1]. This allows increased turbine inlet temperature thereby increasing engine efficiency and power-density. However, particulate entrainment into gas turbine engines (GTEs) for fixed wing and vertical lift aircraft is a significant challenge for both military and civilian missions (see Fig. 1). In the past, this has primarily resulted in erosive damage from hard particulates, i.e. foreign object damage (FOD). Modern GTEs typically have erosion-resistant coatings to improve durability and reduce the operational impact of FOD. However, modern gas turbine engines operate at significantly higher temperatures (at or above 1500 °C) for improved efficiency and increased power density. This increase in operating temperatures has given rise to a new problem for military aircraft engines and power generation gas turbines. Hot tribo-corrosion and deposition from sand, dust, salt, and ash are seen in GTE hot-section components. Fig. 2 shows high-pressure turbine (HPT) components damaged from sand in an engine test conducted by ARL and NAVAIR, as part of a round-robin evaluation of thermal barrier coatings (TBCs).

Fig. 1 Dust cloud during Helicopter take-off, landing or hovering operations over sandy terrain.

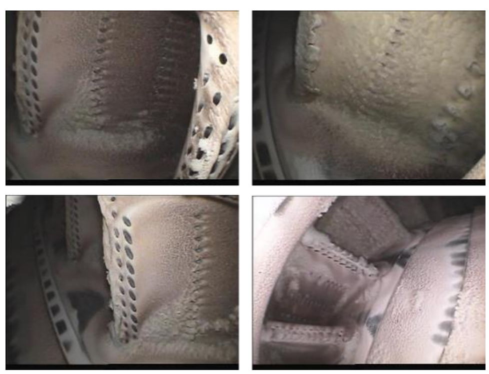

Fig. 2 High-pressure turbine components with sand deposits from an engine ground test showing molten sand adherence and CMAS build-up.

The need for engine components to endure polluted air and perform robustly under multi-domain adverse environments makes it a necessity for aircraft design improvements. Civilian aircraft operating in densely populated and desert regions encounter dust clouds that degrade the gas turbine engines significantly. In addition, aircraft flying through even diffuse volcanic ash clouds can undergo similar engine degradations, as shown in Fig. 3 [2]. The need for aircraft to avoid severe volcanic ash clouds generated by volcanic eruptions in 2010 is estimated to have cost the global economy between $3.3 – 5 billion USD [3, 4]. Effectively small/fine particulates (such as sand, dust, and/or ash) can pass through the cold-section, enter the combustor where the particulates undergo phase transformations and melt, impinge on the high-pressure turbine components, adhere to the protective TBCs, infiltrate into these porous coatings, and solidify into a glassy coating where they can continue to react with and degrade the TBC material [1, 5-10]. The infiltration of the glassy calcia-magnesia-alumino-silicate (CMAS) materials into the TBCs can lead to spallation of the coating and a significant knockdown on engine life. In addition, the adherence of CMAS can lead to significant build-up on the blade/vane coating that may block air-flow passages, leading to engine surge and catastrophic failure of the engine. The need for military vehicles that perform robustly under multi-domain adverse environments makes it a necessity that rotorcraft and the powering engines be able to withstand such harsh sand/dust/ash ingestion and attack. Many rotorcraft turbo-shaft engines are equipped with inlet (also called inertial) particulate separators (IPS), which filters out over 95% of the large particulates (> 100 µm) entering the engine inlet air duct, but these systems are not as effective in filtering out small particulates (< 100 µm). Additionally, the IPS design solution comes with inherent parasitic inlet pressure loss that has bearing on the overall engine power output. Electrostatic particle separators which can remove small particles are either too heavy or can cause high inlet pressure loss which prohibits the use of such devices in helicopters. Hence, a materials solution, such as a sandphobic thermal/environmental barrier coating (T/EBC) [11-18], is needed to mitigate the adherence of small molten particulates and the resultant infiltration of CMAS into the porous TBCs protecting the hot-section components. For example, small sand particulates (< 50 µm) will melt even during much smaller combustor residence times which are typically in the order of micro-seconds [14, 15]. Also, multiple impacts from non-spherical particulates tend to cause more damage, resulting in a nucleation site for subsequent CMAS deposition, than a comparably-sized spherical particle [16-18].

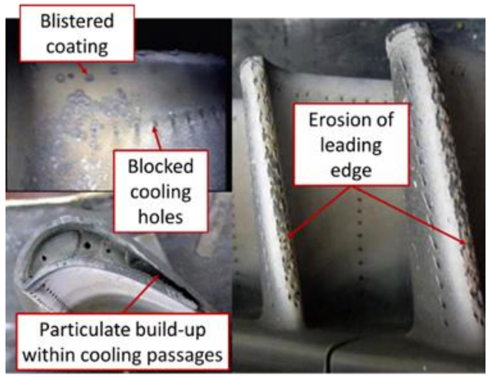

Fig. 3 Damage from a diffuse volcanic ash cloud to the HPT components of a CFM56 engine [2].

In order to advance the gas turbine engine technology for better efficiency and power-density, new blade materials and novel thermal barrier and sand resistant coatings are continually being explored. The development of uncooled turbine blades and other hot section components will be enabled in gas turbines with the advent of new high temperature engine materials, such as ceramic matrix composites (CMCs) or ultra-high temperature composites (UHTCs). SiC-SiC CMC material is currently emerging as a strong alternative material for Ni-superalloy components due to its low density (1/3 density of Ni superalloy) and higher operating temperature capability. However, these SiC-SiC CMC material is highly susceptible to material recession damage caused by water vapor present in the combustion byproducts. Additionally, current research indicates these materials also undergo cracking and spallation under the presence of CMAS. To summarize, the gas turbine research community is continually in search of durable sand-tolerant thermal/environmental barrier coatings both for the currently technology Ni-superalloy based substrates and the emerging SiC-SiC based substrates. A systematic sand-phobic development effort is described in this paper for both TBC for Ni-superalloy based substrates, and for T/EBC for SiC-SiC CMC based substrates. This research consists of (a) high-fidelity multi-phase computational framework, (b) detailed parameter maps of the governing T/EBC properties needed to attain non-reactive, non-wetting behavior that would inhibit CMAS attack and build-up, (c) developing T/EBCs with non-reactive, non-wetting behavior using novel material compositions developed by scalable air plasma spraying (APS) techniques, (d) developing protocols and/or standards for quantifying "CMAS-phobic" (or sandphobicity) behavior and associated environmental impacts that include impact of materials solutions and manufacturing, and vehicle performance with new coating solutions, and (e) a life cycle model to understand the effect of CMAS attack on coating/ engine life reduction and the effect of new coating solutions on hot section components' life. These research efforts that are in progress are described in detail in the coming sections of this paper.

III. High-Fidelity Multi-phase Computational Framework

The project team has developed high-fidelity computational fluid dynamic models to predict multiphase turbulent flow transport, particle collisions, impingement, and wettability behavior of CMAS media in a novel multi-scale framework. This computational framework includes models describing the physics at a range of scales from the mesoscale in viscous flow region near a solid surface, to the large characteristic scales in turbulent flow. To investigate the underlying physics of surface wettability, the multiphase hydrodynamics open-source code Basilisk [19] was adopted in this work. Basilisk is an adaptive Cartesian solver for the Navier-Stokes equations that discretizes the computational domain using a structured grid of finite volumes that can be either uniform or non-uniform. The liquid-gas interface is modeled using a volume of fluid (VoF) approach along with the piecewise linear interface calculation (PLIC) method to reconstruct the interface within each cell. Further, the interface curvature is estimated from the volume fraction using the height-functions method. Basilisk also features quad and octree adaptive mesh refinement (AMR) capability that is crucial for accurate interface tracking at affordable computational cost.

The modeling of droplet spread on solid surface involves accurately representing the moving contact line fluid dynamics at the intersection of the liquid/gas/solid interphases, also known as the triple point. In classical theory, a stress singularity (Huh-Scriven paradox) arises when solving this problem based on the continuum assumption along with no-slip boundary condition [20]. To address this limitation, multiple approaches have been proposed in the literature based on boundary slip models. In this work, two modeling approaches are implemented in Basilisk to enable the solution of droplet spread and moving contact lines.

A. Navier-slip boundary model

The first approach was to prescribe the Navier-slip boundary condition wherein the slip velocity (u_{slip}) is directly proportional to the shear stress of the fluid at the surface boundary [20]. The slip velocity is given by the following expression.

$$u_{slip} = \lambda \left(\frac{\partial u}{\partial y}\right)_{y=0} \tag{1}$$

Here, λ represent the slip length defined as the theoretical distance away from the wall where velocity goes to zero.

Three-dimensional simulations of a Newtonian droplet impinging on a glass surface are performed and validated using the experimental data given in [25]. In this case study multiphase analysis is conducted using the Navier-slip boundary condition at the solid surface along with the solution of the Navier Stokes Equation. The instantaneous snapshots of a water droplet spreading upon hitting an immiscible smooth glass surface is shown in Fig. 4. The results are compared with the experiments at three different times representing the kinematic (Fig. 4(a)) and the spreading phases (Fig. 4(b)-3(c)).

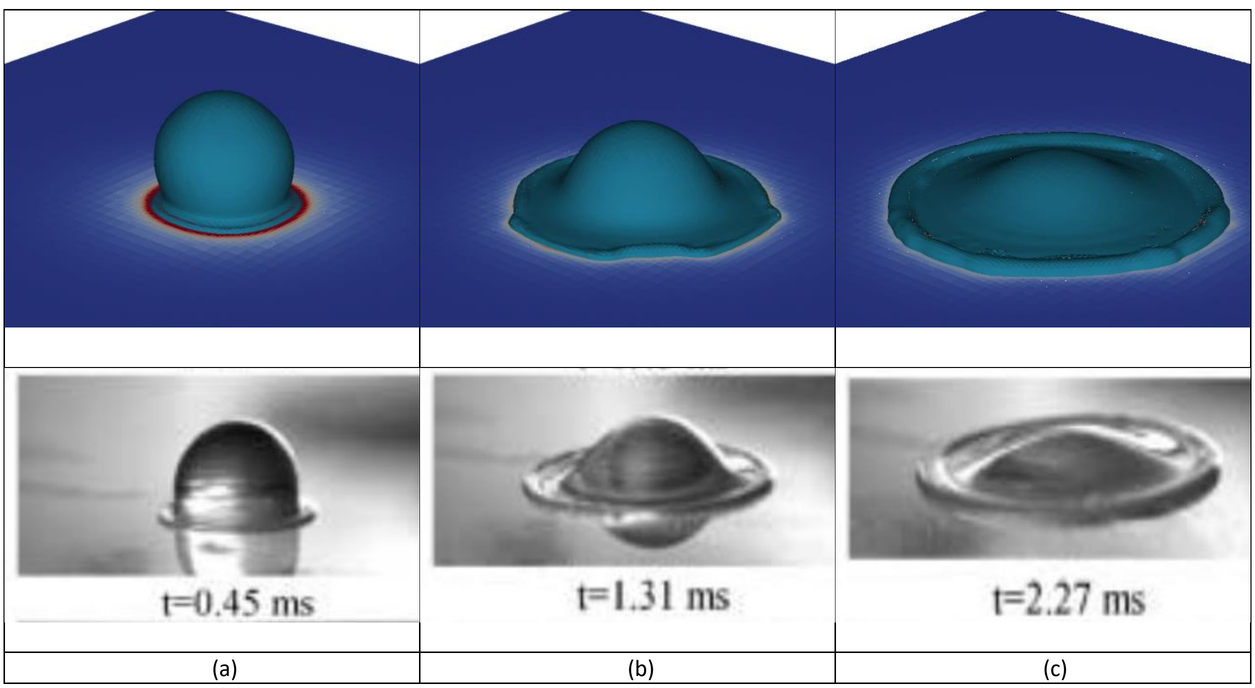

Fig. 4 Comparison of instantaneous snapshots between simulations and the experiments [25] of a Newtonian droplet spreading upon impact at We=58.

In Fig. 5, the evolution of the droplet spread, denoted by the non-dimensional parameter spread factor is shown. For the smaller bubble (D=2.71mm), denoted by the black line, the simulation results seem to agree quite well with the experiments. On the other hand, the spread for the larger drop (D=4.9mm), shown in the red line, is under predicted but shows a similar growth rate as that of the experiments.

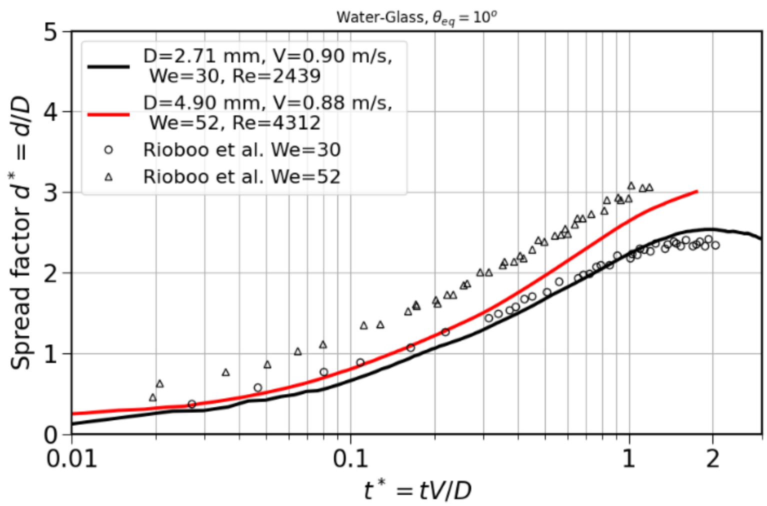

Fig. 5 Time evolution of the Newtonian droplet spread for two different Weber numbers. The black line represents We=30 and the red line represents We=52. The corresponding results from the experiments [25] are represented by the open circles and the open triangles respectively.

B. Dynamic contact angle model

The second approach involved implementation of the dynamic contact angle models to resolve the stress singularity. The two models used in this work are the models proposed by Afkhami, Zaleski and Bussmann et al in [21] (to be referred as AZB09 from here on), and the model proposed by Kistler et al in [22].

The contact angle in AZB09 is modeled using the mathematical description on Eq. 2.

$$cos(\theta_{num}) = cos(\theta_{app}) + 5.63\ Ca\ ln(K/(0.5\Delta)) \tag{2}$$

Here, the apparent contact angle (θ_{app}) is the experimentally observed contact angle at equilibrium and the numerical contact angle (θ_{num}) is the supposed microscopic contact angle that is prescribed as a boundary condition. For a given dynamic viscosity (μ), surface tension (σ) and contact line velocity (u_{cl}), the capillary number (Ca) is defined as $\mu u_{cl}/\sigma$. Here K is a model parameter and Δ is the mesh spacing.

The Kistler's model is empirically determined from the experimental data of Hoffman et al [23]. The numerical contact angle model is given by

$$\theta_{num} = f_H\left(Ca + f_H^{-1}(\theta_{app})\right), \tag{3}$$

where f_H is the Hoffman function given by

$$f_H(x) = cos^{-1}\left\{1 - 2tanh\left[5.16\left(\frac{x}{1 + 1.31x^{0.99}}\right)^{0.706}\right]\right\}. \tag{4}$$

For Ca < 1, the inverse Hoffman function (f_H^{-1}) can be approximated using the Hoffman-Voinov-Tanner law given by [24]

$$f_H^{-1} = \frac{\theta_{app}^3}{c_T}. \tag{5}$$

The constant c_T is set to 72 rad^3.

Sessile droplet simulations with Newtonian fluids were conducting using the dynamic contact angle presented and validated against reference simulation data in Afkhamie et al [21]. The evolution of the non-dimensional drop radius and the dynamic contact angle are shown in Fig. 6. The results show a non-linear behavior with decreasing growth rates evidenced at later times. This indicates that the energy exchange process driving vorticity and instability production near the surface is dominant at the early stages. Both of the models implemented in Basilisk, Kistler and AZB09, are comparable to the reference simulation data shown in Fig. 6.

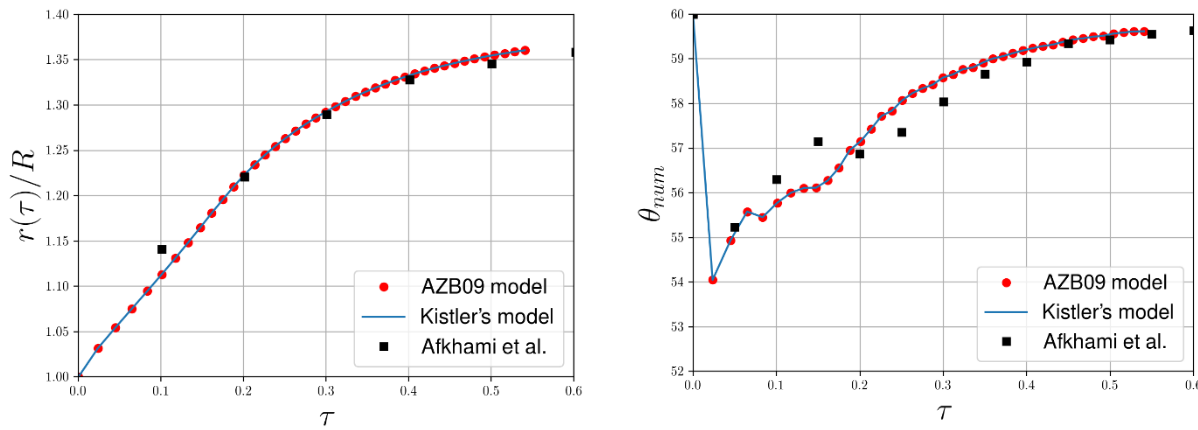

(a) Non-dimensional radius of drop (b) Dynamic contact angle

Fig. 6 The evolution of the droplet radius and the dynamic contact angle are plotted as a function of non-dimensional time. The solid line and the red circles represent the simulation results from the Kistler's and the AZB09 model respectively. The black squares represent data from literature.

The demonstration of the suite of Newtonian wettability models presented here is the foundation towards building a capability able to handle more complex physics to determine a sandphobicity index. Work is underway to experimentally validate the model with measurements from the ARL high temperature contact angle experimental device using CMAS particulates. Images from the facility are shown in Fig. 7. Future work will include results using Newtonian and Non-Newtonian particulates and their chemical interaction with TBC substrates at high temperature.

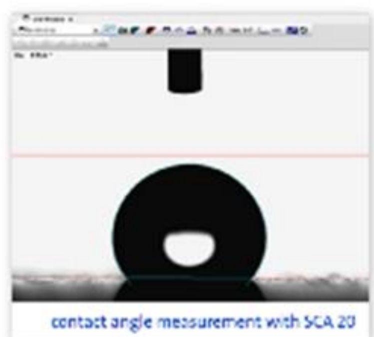

Fig. 7(a) Dynamic Contact angle measurement device **Fig. 7(b) High speed droplet impact test**

IV. Parameter Maps for Desired T/EBC Properties

The identification of primary mechanisms for sand accumulation and its abatement include: (a) surface finish improvement, (b) surface debris 'wetting' reduction/repellant, (c) ablative, and (d) limit infiltration through microstructural tuning. The primary mechanism(s) for sand melt/CMAS infiltration depth, glassification and mitigation are: (a) viscosity and surface tension of the melt (contact angle measurement), (b) operational temperature and surface temperature of the substrate, (c) shape of the inter-columnar gaps (tortuosity factor), (d) CMAS intrinsic strength, CMAS and T/EBC interface adhesion quantification, (e) thermal conductivity and Porosity of T/EBC, (f) size and shape of original sand particulate (spherical vs nonspherical), and (g) impingement velocity and local pressure.

There are three general approaches that researchers have taken to develop CMAS-resistant coatings [12]: (1) impermeable coatings, (2) sacrificial coatings, and 3) non-wetting coatings. CMAS rapidly infiltrates any porous coating regardless of pore morphology [6]. A dense coating impermeable to CMAS is critical to prevent infiltration and spallation of the TBC. The primary approach to creating an impermeable CMAS layer is by coating with a dense, non-reactive material. Primary methods for abating sand accumulation include surface finish improvement, surface debris 'wetting' reduction/repellant, ablative or thin film bleed air interference with the sand settlement, and microstructural tuning to limit infiltration. These mechanisms are investigated to identify the governing parameters via computational methods developed and experimental methods for sand melt/ CMAS infiltration depth, glassification and causal effects that include viscosity and surface tension of the melt (contact angle measurement), operational temperature and surface temperature of the substrate, shape of the inter-columnar gaps (tortuosity factor), CMAS intrinsic strength, CMAS and T/EBC interface adhesion quantification, thermal conductivity and porosity of T/EBC, size and shape of original sand particulate (spherical vs nonspherical). A 'good' TBC has the desired characteristics of low thermal conductivity, similar coefficient of thermal expansion as the substrate material, thermal strain tolerance (during heating and cooling cycles), phase stability, high resistance to fracture and deformation, (i.e. hardness and fracture toughness), ability to survive in an oxidizing atmosphere, low density and to be thermodynamically compatible with the bond coat oxide [26]. YSZ (Ytttria Stabilized Zirconia) is the current state-of-the-art TBC technology and has been widely used in gas turbine engines because of its unique combination of thermal and mechanical properties. However, YSZ has very poor resistance to CMAS. CMAS rapidly infiltrates into porous YSZ coating where it leaches yttria from the coating, thus destabilizing and transforming the favorable tetragonal zirconia to the monoclinic and cubic phases [27]. The CMAS permeates into the coating-bond coat interface and recrystallizes during thermal cycling causing spallation of the entire coating. Rare earth oxides have generated significant interest as potential TBCs for CMAS-resistant thermal barrier coatings in gas turbine environments [28]. Kramer et al. discovered that GZO rapidly reacted with the CMAS to form apatite and fluorite phases sealing the remaining TBC from further CMAS infiltration [29]. However, the relatively low fracture toughness [30, 31] and poor erosion resistance [32] of GZO has prevented its widespread application.

While the industry and research community are trying to find a perfect CMAS-resistant TBCs for Ni-based superalloy materials, there has been a new generation of emerging Ceramic Matrix Composite (CMC) materials that are advancing to replace Ni-superalloy based propulsion materials due to increased demands for fuel efficiency and power-density. Lightweight silicon carbide based (e.g. SiC-SiC) CMCs are currently leading candidates to replace the three times heavier nickel-based superalloys for hot section components used in advanced gas turbine engines. Unfortunately, exposures of these materials to high temperature combustion environments with water vapor limits the effectiveness of thermally grown silica scales in providing protection from oxidation and component recession during service. Hence, environmental barrier coatings (EBCs) are necessary to protect the underlying ceramic substrate from environmental attack. A significant challenge for prime reliant EBC systems is the common occurrence of foreign particles in the engine during service. The size and composition of the particles, along with their temperature during interaction with the protective EBC dictates the prevalent damage mechanism to the coating system, where molten CMAS and solid particle (e.g. erosion and impact) attack are both of high concern. The scientific approaches may include self-regenerative layered or graded environmental barrier coatings deposited upon functionally gradient CMC bulk material with relatively low thermal conductivity, high thermomechanical strain tolerance, and resistance to molten/semi-molten particulate adherence and infiltration. The incorporation of such techniques will significantly enhance the durability of T/EBC coated SiC-SiC CMCs leading to an extension of the component lifetime.

The emerging generation T/EBCs for CMC are rare earth (RE) silicates and disilicates. These T/EBCs require a bond coat to ensure adequate adhesion with the substrate and reduced CTE (coefficient of thermal expansion) mismatch that can often lead to coating failure via delamination or spallation. Mullite-based bond coats have been widely used for EBCs due to their good CTE compatibility with SiC-SiC based CMCs, and good interlayer adhesion due to the presence of Si. A composite HfO_2-Si bond coat has shown promise for providing a compromise between less reactivity with water vapor (HfO_2 is highly tolerant to water vapor attack), while maintaining good adhesion and low CTE mismatch with SiC based substrates. Research work at ARL seeks to understand the effect of various constituent phases and interfaces present in a multi-component T/EBC system on the CMAS infiltration kinetics, under conditions similar to those encountered in a GTE exposed to severe sand ingestion. The T/EBCs investigated so far consist of plasma sprayed top coat with both intersplat porosity (inherent to APS process), as well as vertical cracks that are intentionally introduced to improve damage tolerance. Prolonged exposure to CMAS infiltration may even expose the bond coat to CMAS attack. The rates and possible reactions that may occur on both top coat and bond coat layers are investigated here by exposing the T/EBCs to controlled combustion flow conditions for prolonged exposure intervals that induce CMAS infiltration through the EBC layer(s). Commercially available grades of silicon carbide hexalloys are used as the substrate material instead of expensive SiC-SiC CMC specimens to study performance effectiveness of experimental T/EBCs. An HfO_2-Si composite bond coat, developed by ARL-NASA collaboration, was deposited using APS. Then the binary rare earth disilicate (Yb, $Gd)_2Si_2O_7$ EBC top coat was deposited using APS. Microstructures of as-sprayed (AS) coatings as well as CMAS tested specimens were characterized via SEM and EDS. CMAS infiltration tests are conducted using the ARL's Hot Particulate Ingestion Rig (HPIR). Specimens were exposed to combustion flows with a velocity of 0.5 Ma and temperature of 1550 °C. AFRL-02 sand (surrogate sand to create CMAS) is introduced into the combustion flow at a rate of 1 g/min. Fig. 8 shows a (Yb,Gd)-disilicate T/EBC through a 30 min exposure, sand flow ~ 1 g/min, with gas temperature ~ 1550 °C (~2820 ºF). The sand has formed an interesting accumulation pattern in the flow. The surface of the CMAS is very shiny, which may be indicative of a highly glassified material. Fig. 9 shows ZrO_2-Y_2O_3 based T/EBC systems as sprayed. This solid-solution mixture is promising due to compatible optical basicity with CMAS [33], and is currently under investigation at ARL and in academia [34].

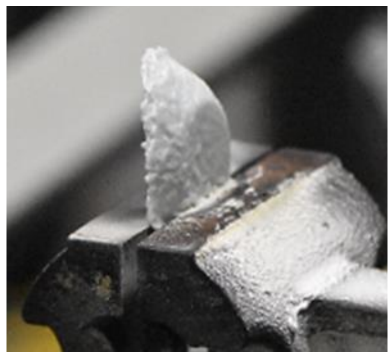

Fig. 8 (Yb, Gd)-disilicated T/EBC with CMAS deposition from a 30 min continuous sand test at the ARL HPIR.

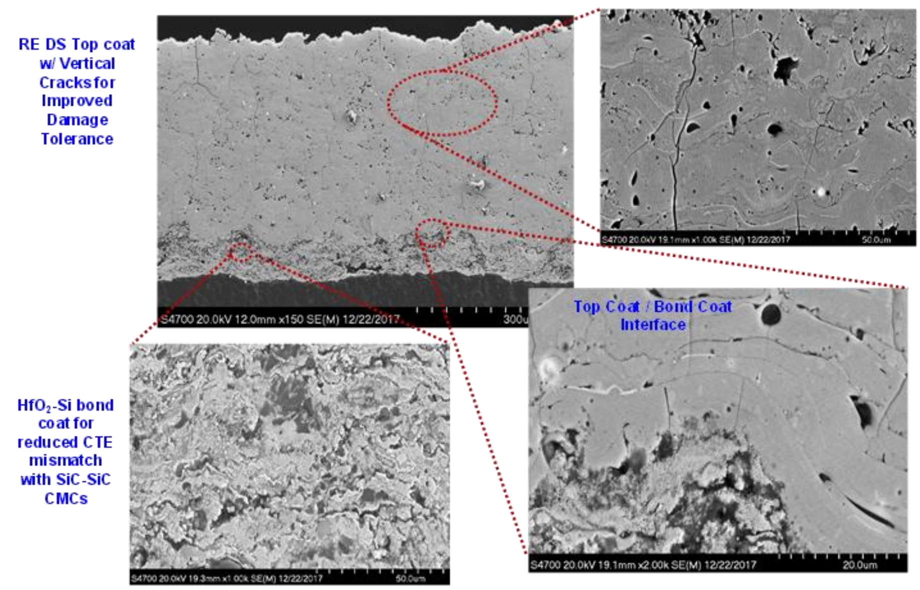

Fig. 9 ZrO_2-Y_2O_3-based T/EBC system in the as-sprayed condition.

The research team is following a systematic approach to innovate physics-informed model-based techniques in developing sandphobic T/EBCs for both Ni-based superalloys and SiC-SiC CMC based gas turbine components. The modeling framework described in the previous section informs T/EBC development on flat panel and curved specimens in terms of the right type of surface morphology for wetting/spreading phobicity, compatibility with substrate in CTE, and the typically needed characteristics like low-k, erosion resistance, and fracture toughness. The spray processing parameters will be optimized for appropriate porosity/densification, coating thickness, and surface roughness. Additionally, fundamental understanding of the feedstock materials (i.e. powders) is critical to the effective development of these material systems and optimization of the processing conditions. Powder characterization will be accomplished via laser diffraction analysis of the particle size and distribution, scanning electron microscopy (SEM) for surface features and morphology, and x-ray diffraction (XRD) for chemistry and phase analysis. The developed coatings will undergo systematic test evaluations, initially at the coupon level and finally at the component level as described in the next section. Before selecting the candidate coatings for the component level experimental evaluations, environmental impact assessments will be conducted while checking their ability to resist CMAS infiltration and accumulation on specimens under engine relevant operating conditions. At the end of this project, the research team will also conduct life cycle framework and sustainability analysis for the most promising coating candidate selections.

V. Experimental Evaluations

ARL is conducting an in-depth experimental evaluation to study CMAS adhesion mechanisms, sand sintering, and CMAS infiltration improving upon prior research efforts [35-38]. The baseline test specimens include (1) Inconel 718 disk with YSZ top coat, or graded Gd_2O_3/YSZ (from previously developed and U.S patent-filed TBC that shows promising sand tolerance [39]) and NiCoAlY bond coat, and (2) SiC/SiC CMC substrate with RE-disilicate T/EBC and mullite bond coat. Due to high cost of state-of-the-art SiC/SiC CMC material specimens, initial work is performed using monolithic SiC disks to assess the coatings.

A. Coupon level experiments

One-inch circular disk specimens are prepared and will be tested at the required engine relevant conditions. Initial experiments include isothermal furnace testing of these one-inch specimens with wet slurry sand paste under high temperature and pressure conditions. AFRL02, a surrogate sand developed by AFRL and University of Dayton Research Institute (UDRI) to produce consistent CMAS chemistry is used. The sand adhesive force is measured using an adhesion tester (shown in Fig. 11). Then the separated specimens are microscopically analyzed for sintering and infiltration characterizations. The key evaluation success criteria from these tests would be (1) CMAS adhesion force estimation (weaker force would mean easy CMAS flake-off and possible purging due to transient engine flow velocities combined with blade film cooling flows), and (2) minimal CMAS build-up and infiltration into the coating. ARL also conducts particle impingement erosion tests on these coated specimens using the Jet Erosion Rig shown in Fig. 12. The Jet Erosion Rig (shown in Fig. 12) is used to test the coated specimens at erodent impingement velocities ranging from 30 m/s to 150 m/s with different incidence angles and the specimen heated up to ~1050 °C. Erodent particles such as alumina (used in ASTM standard erosion test) as well as sand are used to conduct this testing. The key evaluation criteria for this test is the coating survivability under particulate impingement exhibiting good coating erosion resistance and fracture toughness.

(a) (b)

Fig. 11 (a) YSZ coated button cell samples, (b) Adhesion tester prep with the button cells and sand slurry post-sintered in the furnace

Fig. 12 ARL Jet Erosion Rig

In order to assess the wettability characteristics of the coated specimens, the project team will conduct sessile drop tests of sand melt at ambient temperature and sand melt test at elevated temperatures on the coating surface of specimens. The contact angle measurement will be made using a high temperature DataPhysics - Dynamic Contact Angle Measurement hardware (shown in Fig. 13) capable of heating the contact surface up to a maximum temperature of 1800 °C. The molten sand wetting and spreading behavior on T/EBC surface from baseline and samples with surface treatments will be characterized. The resistance to spreading of molten sand droplet will be assessed using this equipment and then incorporated into sandphobicity index assessments for candidate coatings and their surface treatments. The surface roughness of the coating will be evaluated using a Zeiss confocal microscope.

Fig. 13 DataPhysics - High Temperature Contact Measurement Unit capable of reaching 1800 °C

Fig. 14 ARL S-MART Rig

The coated specimens are then tested using a Sand-modified ablation rig test (S-MART) as shown in Fig. 14. The Sand-modified ablation rig test (S-MART) consists of an oxy-fuel torch positioned over a motorized rotary stage. The torch is capable of producing gas temperatures up to 3480 °C, while specimen surface temperatures are monitored by an optical pyrometer. An aqueous sand slurry is applied to the surface of the coatings and then exposed to an oxy-propane flame for 5cycles of 3min in the flame and 3min out of the flame with target specimen surface temperature maintained at 1300 °C, as measured by an optical pyrometer. This test allows up to seven (7) coatings to be tested simultaneously while exposed to sand and heat. The tested coatings are visually inspected for damage such as cracking and spallation. Coatings with no visible damage become eligible for more vigorous testing via the Hot Particulate Ingestion Rig (HPIR) shown in Fig. 15. Material micro-structural evaluations are also done to assess the coating integrity post-test. After the down-selection of candidate coatings from the S-MART, the specimens are then tested using HPIR which simulates gas turbine engine relevant flow velocities and temperatures. The HPIR test setup is capable of sand and water ingestion. The surrogate sand (AFRL02) is ingested into the combustor where it melts and flows in the hot gas stream impinging on the specimen target. Sand ingestion will be used for Ni-superalloy specimens with TBCs, whereas Si-SiC specimens with E/TBCs will be tested with both sand and water ingestion to evaluate material recession along with CMAS resistance. The tested specimens will undergo rigorous post-test examinations such as (1) Hardness testing via micro- and nano-indentation, (2) Porosity (typically measured through metallographic examination of the cross section via optical microscopy), (3) Coating thickness (measured by metallographic examination of the cross section via optical or electron microscopy), (4) Infiltration depth (measured by metallographic examination of the cross section via optical and/or electron microscopy), (5) Grain structure (typically examined via electron backscattered diffraction (EBSD) in the scanning electron microscope (SEM)), and (6) Phase identification and quantification (typically measured via x-ray diffraction and/or EBSD). The success criteria for the selected coatings would be no cracks/damages/spallations, minimal chemical interaction with CMAS and minimal CMAS infiltration into the coating.

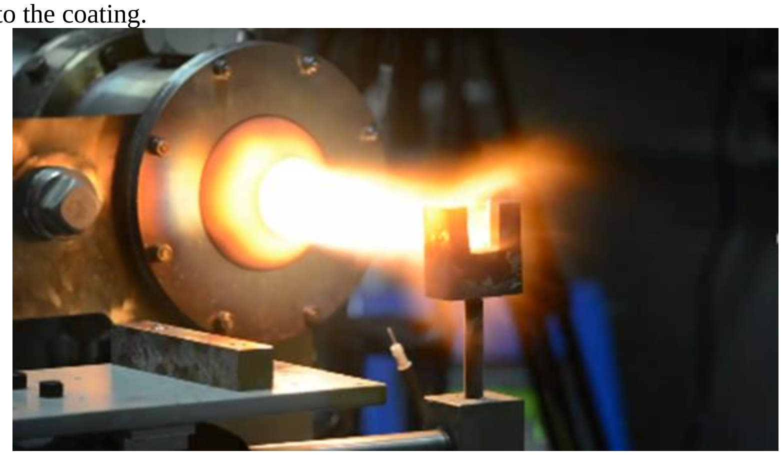

Fig. 15 ARL Hot-Particulate Ingestion Rig (HPIR)

B. Component level experimental demonstration

Finally after successful candidate coatings are selected from the coupon level experimental evaluations, and after assessing the environmental impact of these selected coatings, the promising candidate coatings will be applied to a typical turbine high pressure turbine (HPT) component such as a vane (or turbine rotor blade) or a shroud ring segment for component level test evaluations. It is proposed that for T/EBC development of a SiC-SiC based gas turbine engine component, a shroud ring segment made of SiC-SiC CMC material will be used since it is cheaper and easier to obtain. However, for metallic turbine nozzle vane or rotor blade evaluation, a typical High Pressure Turbine (HPT) nozzle vane or rotor blade from an OEM made of single crystal Ni-superalloy material will be used. These components are shown in Fig. 16.

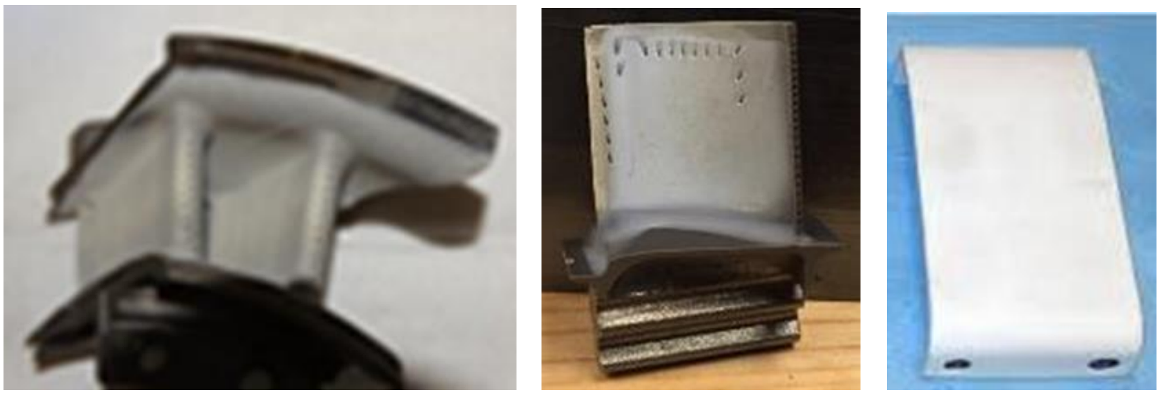

(a) HPT nozzle vane **(b) HPT rotor blade** **(c) HPT shroud segment** (Courtesy: kundoc.com)

Fig. 16 HPT components for sandphobic T/EBC demonstration

The component test demonstration tests will be conducted for thermal durability and sand tolerance evaluations. It should be noted that sand particle loading in the test evaluations is based on rotorcraft take-off/landing or hover flight conditions in typical sandy terrain with sand ingestion rates of 10lbs/hr to 40lbs/hr at engine inlet with a built-in inlet particle separator.

Form the above demonstration tests, validated promising new high durability/sandphobic T/EBCs for a realistic metallic turbine nozzle vane (or turbine blade) and for a realistic SiC-SiC turbine shroud ring segment will be obtained. Promising coatings evaluated will be rank ordered according to the sandphobicity index developed from the previous steps. In addition, consideration will be given to health effects of coating material chemistry and lifecycle assessment and sustainability characteristics of successful coating candidates.

VI.Environmental Impact and Lifecycle Assessment

Using a combination of published literature, knowledge of federal and state regulations, coatings down-selected from the previous research steps will be analyzed for their impact on human health and environmental impacts. In addition, the raw materials and the processing conditions necessary to develop/produce the down-selected coatings will also be evaluated for potentially harmful by-products. This analysis will provide the framework for a go/no go criteria (see Fig. 10) on the potential impact of the developed coatings to human health and the environment. The effects of coatings on the environment as a whole including long-term exposure to high temperature hot gases and combustion by-products during engine operations will also be analyzed as part of this research. All these assessments will be summarized for the selected coating solutions in future publications. Based on these assessments on the human health and environmental impacts, promising coating solutions will be down-selected and reported. In addition, using the data generated during testing, along with the actual materiel costs, a baseline framework for an effective lifecycle inventory scheme will be developed. The resources, such as databases, models, and software tools available from DoD and EPA (Environmental Protection Agency) will be used to do life cycle assessment and sustainability analysis for the most promising coating solutions from this research project. The overall sustainability analysis frame work will include initial life cycle cost estimation and life cycle assessment feeding into sustainability analysis. All of these assessments and estimations will be used in making the right selections for the coating solutions recommended through this research.

VII. Summary and Future Work

This research and development is currently ongoing. The results are planned to be published in stages as the project progresses. The preliminary physics-based modeling & simulation methodologies for the CMAS wetting/spreading mechanisms have been developed and being verified currently. The experimental test methods, thermal spray and material characterization techniques have been developed and refined through prior TBC research & development at ARL. Prior post-test material analysis along with prior simulation and experimental evaluations have helped identification of governing parameters for CMAS mitigation to some extent and enabled the research team to file a patent application for a sandphobic coating that is promising for Ni-superalloy based vanes/blades that can be used in the hot-sections of future gas turbine engines. However, these governing parameters need to be further studied through this ongoing research to develop a model-based "Sandphobicity Index" that can be used to design T/EBCs for future gas turbine hot-section components. In future, the sandphobic coatings developed under this current research program will be evaluated by a full ground engine sand ingestion test and possibly a flight test. The optimized enhanced T/EBC sandphobic coating for CMC and single crystal Ni-based superalloys will be incorporated onto test components (e.g. shroud, vanes, blades) for full scale engine test validation to TRL-6 or higher in collaboration with gas turbine engine manufacturers. The resulting technology will enable significantly enhanced time-on-wing/durability of hot section components of future advanced engines with high turbine inlet temperatures operating in particle laden environments. Both military and commercial aircraft applications are likely to benefit from this sandphobic coating technology research.

Acknowledgment

The authors acknowledge the support from received from DoD's Strategic Environmental Research and Development Program (SERDP) for this research. The research reported in this document is being performed in connection with contract/instrument W911QX-16-D-0014 with the U.S. Army Research Laboratory. The authors are thankful to Dr. Robin Nissan (SERDP Program Manager) and Mr. Braxton Lewis (Principal Scientist, SERDP) for their support to this SERDP project# WP20-1281. The views and conclusions contained in this document are those of the authors and should not be interpreted as representing the official policies or positions, either expressed or implied, of the U.S. Army Research Laboratory or the U.S. Government.

References

[1] Levi, G. G., Hutchinson, J. W., Vidal-Sétif, M. H., and Johnson, C. A., "Environmental degradation of thermal-barrier coatings by molten deposits," MRS Bulletin, vol. 37, pp. 932-941, 2012.

[2] Grindle, T. J., Burcham, J., and Frank W., "Engine damage to a NASA DC-8-72 airplane from a high-altitude encounter with a diffuse volcanic ash cloud," ed: National Aeronautics and Space Administration, 2003.

[3] Mazzocchi, M., Hansstein, F., and Ragona, M., "The 2010 volcanic ash cloud and its financial impact on the European airline industry," CESifo Forum, vol. 11, pp. 92-100, 2010.

[4] O. Economics, "The economic impacts of air travel restrictions due to volcanic ash," Oxford Economics, Oxford, UK2010.

[5] Vidal-Setif, M. H.., Chellah, N., Rio, C., Sanchez, C., and Lavigne, O., "Calcium-magnesium-alumino-silicate (CMAS) degradation of EB-PVD thermal barrier coatings: Characterization of CMAS damage on ex-service high pressure blade TBCs," Surface & Coatings Technology, vol. 208, pp. 39-45, Sep 15 2012.

[6] Krämer, S., Yang, J., Levi, C. G., and Johnson, C. A., "Thermochemical Interaction of Thermal Barrier Coatings with Molten CaO–MgO–Al2O3–SiO2 (CMAS) Deposits," Journal of the American Ceramic Society, vol. 89, pp. 3167-3175, 2006.

[7] Padture, N. P., Gell, M., and Jordan, E. H., "Thermal Barrier Coatings for Gas-Turbine Engine Applications," Science, vol. 296, pp. 280-284, 2002.

[8] Borom, M. P., Johnson, C. A., and Peluso, L. A., "Role of environmental deposits and operating surface temperature in spallation of air plasma sprayed thermal barrier coatings," Surface & Coatings Technology, vol. 86-87, pp. 116-126, 1996.

[9] Smialek, J. L., Archer, F. A., and Garlick, R. G., "Turbine airfoil degradation in the persian gulf war," JOM, vol. 46, pp. 39-41, December 01 1994.

[10] Miller, R. A., "Current status of thermal barrier coatings," Surface & Coatings Technology, vol. 30, pp. 1 - 11, January 1987.

[11] Leiter, P., "Development of an environmental barrier coatings to mitigate CMAS attack," MSc, School of Industrial and Information Engineering, Cranfield University / Politecnico Milano, 2016.

[12] Rai, A. K., Bhattacharya, R. S., Wolfe, D. E., and Eden, T. J., "CMAS-Resistant Thermal Barrier Coatings (TBC)," International Journal of Applied Ceramic Technology, vol. 7, pp. 662-674, 2010.

[13] Li, L., Hitchman, N., and Knapp, J., "Failure of Thermal Barrier Coatings Subjected to CMAS Attack," Journal of Thermal Spray Technology, vol. 19, pp. 148-155, January 01 2010.

[14] Walock, M. J., Barnett, B. D., Ghoshal, A., Murugan, M., Swab, J. J., Pepi, M. S., Hopkins, D., Gazonas, G., Rowe, C., and Kerner, K., "Micro-scale sand particles within the hot-section of a gas turbine engine," in Mechanical Properties and Performance of Engineering Ceramics and Composites XI: Ceramic Engineering and Science Proceedings. vol. 37, J. Salem and D. Singh, Eds., ed: American Ceramics Society, 2017.

[15] Murugan, M., Ghoshal, A., Nieto, A., Walock, M. J., Bravo, L., Jain, N., Pepi, M., Swab, J., Zhu, D., Pegg, R. T., Rowe, C., and Kerner, K., "Prevention of molten sand attack on thermal barrier coatings for rotorcraft turbine blades - a round robin test evaluation," in AHS International 74th Annual Forum and Technology Display, Phoenix, AZ, 2018.

[16] Murugan, M., Ghoshal, A., Walock, M., Nieto, A., Bravo, L., Barnett, B., Pepi, M., and Kerner, K., "Sand particle-induced deterioration of thermal barrier coatings on gas turbine blades," Advances in Aircraft and Spacecraft Science, vol. 4, pp. 37-52, 2017.

[17] Murugan, M., Ghoshal, A., Walock, M., Nieto, A., Bravo, L., Barnett, B., Pepi, M., Swab, J., Pegg, R. T., Rowe, C., Zhu, D., and Kerner, K., "Microstructure Based Material-Sand Particulate Interactions and Assessment of Coatings for High Temperature Turbine Blades," in Proceedings of the ASME Turbo Expo: Turbine Technical Conference and Exposition, GT2017-64051, 2017.

[18] Ghoshal, A., Murugan, M., Walock, M., Nieto, A., Barnett, B., Pepi, M., Swab, J., Zhu, D., Kerner, K., Rowe, C., Shiao, C.-Y., Hopkins, D., and Gazonas, G.A., "Molten particulate impact on tailored thermal barrier coatings for gas turbine engine," Journal of Engineering for Gas Turbines and Power, vol. 140, 2018.

[19] Popinet, S. (2009). An accurate adaptive solver for surface-tension-driven interfacial flows. Journal of Computational Physics, 228(16), 5838-5866.

[20] Bonn, D., Eggers, J., Indekeu, J., Meunier, J., and Rolley, E. (2009). Wetting and spreading. Reviews of modern physics, 81(2), 739.

[21] Afkhami, S., Zaleski, S., and Bussmann, M. (2009). A mesh-dependent model for applying dynamic contact angles to VOF simulations. Journal of computational physics, 228(15), 5370-5389.

[22] Kistler, S. F. (1993). Hydrodynamics of wetting. Wettability, 6, 311-430.

[23] Hoffman, R. L. (1975). A study of the advancing interface. I. Interface shape in liquid—gas systems. Journal of colloid and interface science, 50(2), 228-241.

[24] Göhl, J., Mark, A., Sasic, S., and Edelvik, F. (2018). An immersed boundary based dynamic contact angle framework for handling complex surfaces of mixed wettabilities. International Journal of Multiphase Flow, 109, 164-177.

[25] Rioboo, R., Marengo, M., and Tropea, C. (2002). Time evolution of liquid drop impact onto solid, dry surfaces. Experiments in fluids, 33(1), 112-124.

[26] Clarke, D. R., and Phillpot, S. R., "Thermal barrier coating materials," Materials Today, vol. 8, pp. 22-29, 2005/06/01/ 2005.

[27] Naraparaju, R., Schulz, U., Mechnich, P., Döbber, P., and Seidel, F., "Degradation study of 7wt.% yttria stabilised zirconia (7YSZ) thermal barrier coatings on aero-engine combustion chamber parts due to infiltration by different CaO–MgO–Al2O3–SiO2 variants," Surface and Coatings Technology, vol. 260, pp. 73-81, 2014/12/15/ 2014.

[28] Drexler, J. M., Chen, C.-H., Gledhill, A. D., Shinoda, K., Sampath, S., and Padture, N. P., "Plasma sprayed gadolinium zirconate thermal barrier coatings that are resistant to damage by molten Ca–Mg–Al–silicate glass," Surface and Coatings Technology, vol. 206, pp. 3911-3916, 2012/05/25/ 2012.

[29] Krämer, S., Yang, J., and Levi, C. G., "Infiltration-Inhibiting Reaction of Gadolinium Zirconate Thermal Barrier Coatings with CMAS Melts," Journal of the American Ceramic Society, vol. 91, pp. 576-583, 2008.

[30] Vaßen, R., Traeger, F., and Stöver, D., "New Thermal Barrier Coatings Based on Pyrochlore/YSZ Double-Layer Systems," International Journal of Applied Ceramic Technology, vol. 1, pp. 351-361, 2004.

[31] Naraparaju, R., Lau, H., Lange, M., Fischer, C., Kramer, D., Schulz, U., and Weber, K., "Integrated testing approach using a customized micro turbine for a volcanic ash and CMAS related degradation study of thermal barrier coatings," Surface and Coatings Technology, vol. 337, pp. 198-208, 2018/03/15/ 2018.

[32] Mahade, S., Curry, N., Björklund, S., Markocsan, N., Nylén, P., and Vaßen, R., "Erosion Performance of Gadolinium Zirconate-Based Thermal Barrier Coatings Processed by Suspension Plasma Spray," Journal of Thermal Spray Technology, vol. 26, pp. 108-115, January 01 2017.

[33] Krause, A. R., Senturk, B. S., Garces, H. F., Dwivedi, G., Ortiz, A. L., Sampath, S., and Padture, N. P., "$2ZrO_2 \cdot Y_2O_3$ Thermal Barrier Coatings Resistant to Degradation by Molten CMAS: Part I, Optical Basicity Considerations and Processing," Journal of the American Ceramic Society, vol. 97, pp. 3943-3949, 2014.

[34] Krause, A. R., Garces, H. F., Herrmann, C. E., and Padture, N. P., "Resistance of 2ZrO(2)center dot Y2O3 top coat in thermal/environmental barrier coatings to calcia-magnesia-aluminosilicate attack at 1500 degrees C," Journal of the American Ceramic Society, vol. 100, pp. 3175-3187, Jul 2017.

[35] Ghoshal, A., Walock, M. J., Murugan, M., Mock, C. H., Bravo, L., Pepi, M., Nieto, A., Wright, A., Luo, J., Jain, N., Flatau, A., and Frehenbacher, L., “Governing Parameters Influencing CMAS Adhesion and Infiltration into Environmental/Thermal Barrier Coatings in Gas Turbine Engines”, GT2019-92000, Proceedings of ASME Turbo Expo 2019, June 17-21, 2019, Phoenix, Arizona, USA.

[36] Mock, C., Walock, M. J., Wright, A., Nieto, A., Ghoshal, A., Murugan, M., and Pepi, M., “Rare-Earth Oxides Blended with Yttria-Stabilized Zirconia Thermal Barrier Coatings for Improved Resistance to Sand Adherence and Calcia-Magnesia-Alumino-Silicate (CMAS) Infiltration”, GT2019-90395, Proceedings of the ASME Turbo Expo 2019, June 17-21, 2019, Phoenix, AZ, USA.

[37] Bravo, L., Jain, N., Khare, P., Murugan, M., Ghoshal, A., and Flatau, A., “Physical aspects of CMAS particle dynamics and deposition in turboshaft engines”, Journal of Materials Research, vol. 35, 17 (Focus Issue: Sand-phobic T/EBC for Gas Turbine Engines), 2020, https://doi.org/10.1557/jmr.2020.234.

[38] Clara M., Walock, M. J., Ghoshal, A., Murugan, M., and Pepi, M., "Adhesion behavior of calcia–magnesia–alumino–silicates on gadolinia-yttria-stabilized zirconia composite thermal barrier coatings," Journal of Materials Research, 2020, DOI: 10.1557/jmr.2020.184.
[39] Nieto, A., Walock, M. J., Ghoshal, A., Barnett, B. D., Mock, C., Graybeal, M. L., Pepi, M. S., and Murugan, M., US patent application for "Functionally graded sandphobic blended composite coatings," US Patent Application No. 16/748,971, filed 22 Jan 2020.